

Extinction of impurity resonances in large-gap regions of inhomogeneous d -wave superconductors

Brian M. Andersen¹, S. Graser², and P. J. Hirschfeld²

¹*Nano-Science Center, Niels Bohr Institute, University of Copenhagen, Universitetsparken 5, DK-2100 Copenhagen, Denmark*

²*Department of Physics, University of Florida, Gainesville, Florida 32611-8440, USA*

(Dated: November 20, 2018)

Impurity resonances observed by scanning tunneling spectroscopy in the superconducting state have been used to deduce properties of the underlying pure state. Here we study a longstanding puzzle associated with these measurements, the apparent extinction of these resonances for Ni and Zn impurities in large-gap regions of the inhomogeneous $\text{Bi}_2\text{Sr}_2\text{CaCu}_2\text{O}_{8+x}$ superconductor. We calculate the effect of order parameter and hopping suppression near the impurity site, and find that these two effects are sufficient to explain the missing resonances in the case of Ni. There are several possible scenarios for the extinction of the Zn resonances, which we discuss in turn; in addition, we propose measurements which could distinguish among them.

PACS numbers: 74.72.-h, 74.81.-g, 74.25.Jb, 72.10.Fk

I. INTRODUCTION

An understanding of the low doped Mott region of cuprate superconductors remains a key problem in condensed matter physics.¹ It has been proposed that electronic inhomogeneity is crucial for explaining experiments performed in the underdoped regime,² and that the inhomogeneity arises from strong Coulomb repulsion which instigates the formation of spin- and charge density waves, enhanced and pinned by a random potential generated by the doping process, or by external probes which break the translational symmetry. Recent theoretical modelling has shown that several single-particle and two-particle experimental probes can be explained within a scenario where the underdoped superconducting region consists of a d -wave pair state coexisting with a local cluster spin glass phase driven by disorder.³⁻⁷

Scanning tunneling microscopy/spectroscopy (STM/STS) measurements have provided a wealth of detailed local density of states (LDOS) spectra on the surface of $\text{Bi}_2\text{Sr}_2\text{CaCu}_2\text{O}_{8+x}$ (BSCCO), revealing an inhomogeneity in the spectral gap on the nanometer scale.⁸⁻¹¹ Furthermore, the differential conductance has been measured in the vicinity of Zn and Ni substituents for planar Cu.¹¹⁻¹³ Theoretically, the STS spatial conductance pattern produced by the magnetic Ni ion and its resonance energy of $\Omega_0 \simeq \pm 10$ meV can be well described by a combination of potential and magnetic scattering,¹⁴ whereas no consensus has been reached about the proper explanation of the pattern around the Zn impurity, even though the local perturbation caused by the ion should in principle be simpler.¹⁵⁻¹⁸

One way to gain further insight into the nature of the physical state of small-gap versus large-gap regions in cuprate superconductors, is to compare the LDOS near Ni and Zn in these two different environments. Experimentally, it is found that the Ni resonances, which are clearly distinguishable in the small-gap regions, are completely absent in large-gap regions with $\Delta \gtrsim 50$ meV for

optimally doped BSCCO.¹¹ The strength of the resonances which *are* observed does not depend strongly on local gap size, but despite considerable noise appears to anticorrelate slightly with the gap.¹⁹ It was speculated¹¹ that the absence of Ni resonances in large-gap regions is due to the distinct nature of the (pseudogap) phase characterizing these domains. However, phase coherence is not necessary for the creation of impurity resonances; the existence of the pseudogap in the density of states itself should result in well defined impurity resonant states, as found in Ref. 20. Indeed, recent STS measurements on native defects in underdoped single-layer $\text{Bi}_2\text{Sr}_2\text{CuO}_6$ samples have shown that the resonances exist well above the superconducting critical temperature T_c into the pseudogap state.²¹

The LDOS near Zn is characterized by a sharp low-energy resonance around -2 meV in the small-gap regions of optimally doped BSCCO.¹² The resonance weight and width depend strongly on the local environment,^{19,23} and, as in the Ni case,¹¹ the resonances are never observed in the large-gap regions.^{19,23} The temperature dependence of the Zn resonance has been measured within the superconducting state. It was found that the evolution of the peak in the range $30\text{mK} < T < 52\text{K} < T_c$ is consistent with thermal broadening of the peak.²² Within the nonlocal Kondo model for Zn impurities,¹⁶ it was recently argued that a gap-dependent exchange coupling can lead to suppressed Zn resonances in large-gap regions.²⁴ However, this model does not account for the actual spatial variation of the superconducting gap, and it is unclear how to explain the extinction of the Ni resonances. In our view, the question of what causes the extinction of the resonances and whether these effects can indeed be used as probes of pseudogap physics^{13,20} is therefore still open.

For BSCCO materials, a significant part of the observed gap inhomogeneity has been argued to originate from interstitial oxygen dopant atoms;²⁵ detailed theoretical modelling of the LDOS spectra^{26,27} has led to the

remarkable conclusion that the pairing interaction itself seems to be spatially varying in these materials on an atomic scale. This scenario in which the pairing interaction is modulated locally by nearby dopant atoms also explained the origin of the dominant so-called \mathbf{q}_1 peak in the Fourier transformed scanning tunneling spectroscopy (FTSTS) data,^{28,29} and the recently observed pair density wave driven by the structural supermodulation.^{30,31} In addition, it predicted the existence of islands with finite gap above T_c , as recently observed by Gomes *et al.*³² Such islands lead naturally to broadened thermodynamic transitions although this point remains controversial at present.^{33,34}

Here, we show that within the modulated pairing scenario, the absence of Ni resonances in large-gap regions arises naturally when one properly includes the nano-scale inhomogeneity of the superconducting order parameter. This occurs because in-gap impurity resonances in a d -wave superconductor generically borrow their weight from the coherence peaks. In the large-gap regions, these peaks are broad and weak, so they overlap and swamp the weaker resonances located away from the Fermi level. In the small-gap regions, on the other hand, the structures normally referred to as coherence peaks are actually Andreev resonant states of the suppressed order parameter,^{26,35} and their height/width is significantly larger/smaller than in the pure homogeneous case. Thus in the small-gap regions the impurity resonances are well-defined due to their smaller overlap with the continuum. Within the modulated pairing scenario, which reproduces the correlation of the coherence peaks' weight and position with the dopant atoms imaged by STS,²⁵ the presence or absence of Ni resonances is therefore dependent on whether or not interstitial out-of-plane oxygen dopants exist nearby.

We further consider the effect of gap modulation on the Zn resonance near the Fermi level. Here it appears unlikely that the suppression and broadening of the coherence peaks in large-gap regions can alone suppress the impurity resonance because of its weak coupling to the continuum. There is very little experimental data on the variation of the spectral form, weight, and position of

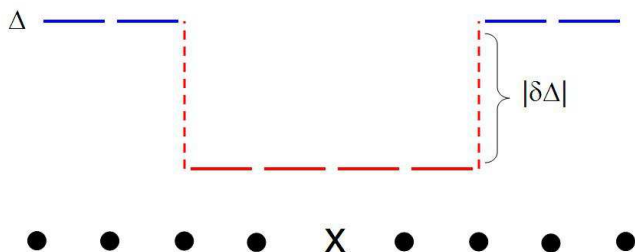


FIG. 1: (Color online) Schematic picture of a small-gap region. Circles are ionic sites, X represents an impurity, and the bonds represent the absolute values of the bond order parameter Δ on bonds in the bulk (top) and in a small gap patch (bottom).

the resonance in correlation with the local gap size, but it appears from what is available^{19,23} that there is considerable dispersion of all these quantities which makes it difficult to extract systematics. Some of this dispersion may simply be due to the well-known very strong interference of near-unitary impurity resonances in a d -wave superconductor.³⁶⁻³⁸ We therefore consider a series of models for the microscopic nature of the Zn potential which might possibly account for the experimental observations, and propose additional experimental tests to distinguish between them.

II. FORMALISM

The starting point of our study is given by the d -wave BCS Hamiltonian

$$\mathcal{H}_0 = \sum_{\mathbf{k}, \sigma} \xi_{\mathbf{k}} \hat{c}_{\mathbf{k}\sigma}^\dagger \hat{c}_{\mathbf{k}\sigma} + \sum_{\mathbf{k}} \left(\Delta_{\mathbf{k}} \hat{c}_{\mathbf{k}\uparrow}^\dagger \hat{c}_{-\mathbf{k}\downarrow}^\dagger + \text{H.c.} \right), \quad (1)$$

where $\xi_{\mathbf{k}}$ denotes the quasiparticle dispersion and $\Delta_{\mathbf{k}} = \frac{\Delta_0}{2} (\cos k_x - \cos k_y)$ is the d -wave pairing gap. In terms of the Nambu spinor $\hat{\psi}_{\mathbf{k}}^\dagger = (\hat{c}_{\mathbf{k}\uparrow}^\dagger, \hat{c}_{-\mathbf{k}\downarrow}^\dagger)$, the corresponding Matsubara Green's function can be expressed as

$$\mathcal{G}^0(\mathbf{k}, i\omega_n) = \frac{i\omega_n \tau_0 + \xi_{\mathbf{k}} \tau_3 + \Delta_{\mathbf{k}} \tau_1}{(i\omega_n)^2 - E_{\mathbf{k}}^2}, \quad (2)$$

where $E_{\mathbf{k}}^2 = \xi_{\mathbf{k}}^2 + \Delta_{\mathbf{k}}^2$, and τ_i denote the Pauli matrices. In real-space, the perturbation due to δ -function potential (magnetic) impurities of strength V_3 (V_0) in the diagonal τ_3 (τ_0) channel is given by

$$\mathcal{H}'_{imp}(\mathbf{r}, \mathbf{r}') = \hat{\psi}_{\mathbf{r}}^\dagger [(V_3 \tau_3 + V_0 \tau_0) \delta(\mathbf{r}) \delta(\mathbf{r}')] \hat{\psi}_{\mathbf{r}'}. \quad (3)$$

Likewise, local modulations in the hopping (δt) or superconducting gap ($\delta \Delta$) enter as

$$\mathcal{H}'_{\delta}(\mathbf{r}, \mathbf{r}') = \hat{\psi}_{\mathbf{r}}^\dagger [-\delta t(\mathbf{r}, \mathbf{r}') \tau_3 - \delta \Delta(\mathbf{r}, \mathbf{r}') \tau_1] \hat{\psi}_{\mathbf{r}'}. \quad (4)$$

To obtain the resulting LDOS as a function of position and energy, one needs to determine the full Green's function $\mathcal{G}(\mathbf{r}, i\omega_n)$ given by the Dyson equation

$$\mathcal{G}(\mathbf{r}, \mathbf{r}') = \mathcal{G}^0(\mathbf{r} - \mathbf{r}') + \mathcal{G}(\mathbf{r}, \mathbf{r}'') \mathcal{H}'(\mathbf{r}'', \mathbf{r}''') \mathcal{G}^0(\mathbf{r}''' - \mathbf{r}'), \quad (5)$$

where $\mathcal{H}' = \mathcal{H}'_{imp} + \mathcal{H}'_{\delta}$, and summation over repeated indices is implied. Thus, by calculating the matrix elements of $\mathcal{G}^0(\mathbf{r}, i\omega_n) = \sum_{\mathbf{k}} \mathcal{G}^0(\mathbf{k}, i\omega_n) e^{i\mathbf{k} \cdot \mathbf{r}}$ the remaining problem is that of a matrix inversion. The solution is presented in terms of the \mathcal{T} -matrix

$$\mathcal{G}(\mathbf{r}, \mathbf{r}') = \mathcal{G}^0(\mathbf{r} - \mathbf{r}') + \mathcal{G}^0(\mathbf{r} - \mathbf{r}'') \mathcal{T}(\mathbf{r}'', \mathbf{r}''') \mathcal{G}^0(\mathbf{r}''' - \mathbf{r}'). \quad (6)$$

The poles of the \mathcal{T} -matrix, or equivalently, the zeros in the determinant of $(1 - \mathcal{H}' \mathcal{G}^0)$, determine the bound state energies. The total (spin summed) LDOS is given by

$$N(\mathbf{r}, \omega) = (-1/\pi) \text{Im} [\mathcal{G}_{11}(\mathbf{r}, \mathbf{r}, \omega) + \mathcal{G}_{22}(\mathbf{r}, \mathbf{r}, -\omega)]. \quad (7)$$

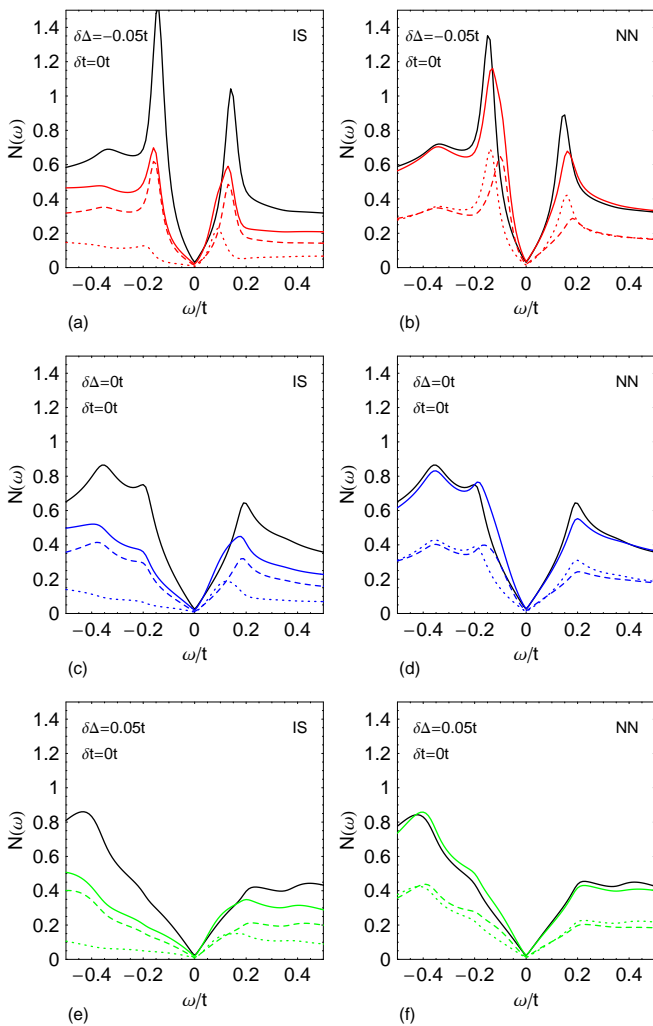


FIG. 2: (Color online) LDOS in a d -wave superconductor with a Ni impurity at the center of a 5×5 patch of (a-b) suppressed ($\delta\Delta = -0.05t$), (c-d) constant ($\delta\Delta = 0$) and (e-f) enhanced ($\delta\Delta = +0.05t$) superconducting gap. The Ni potentials used for this study are $V_3 = -0.8t$, $V_0 = 0.6t$. The figures in the left column (a,c,e) show spectra on the impurity site (IS) itself, while right column (b,d,f) represents nearest neighbor (NN) sites. In each case, the solid black curve shows the LDOS on the site in question in the absence of the impurity, the solid color curve indicates the total LDOS with the impurity, and the dashed and dotted lines show the spin resolved LDOS for up and down spins, respectively.

In explicit calculations we use the band $\xi_{\mathbf{k}} = -2t(\cos k_x + \cos k_y) - 4t' \cos k_x \cos k_y - \mu$ with a d -wave order parameter $\Delta_{\mathbf{k}} = \frac{\Delta_0}{2}(\cos k_x - \cos k_y)$. To model the Fermi surface in the cuprates we take $t' = -0.35t$ and $\mu = -1.1t$, with energy measured in units of nearest neighbor hopping t . We also choose $\Delta_0 = 0.2t$. The modulations in the hopping are included on the bonds near the impurity site assuming maximum modulations δt on the nearest neighbor bonds, with a Gaussian decay on other bonds with decay length of one lattice constant. This is roughly consistent with the renormalization of the

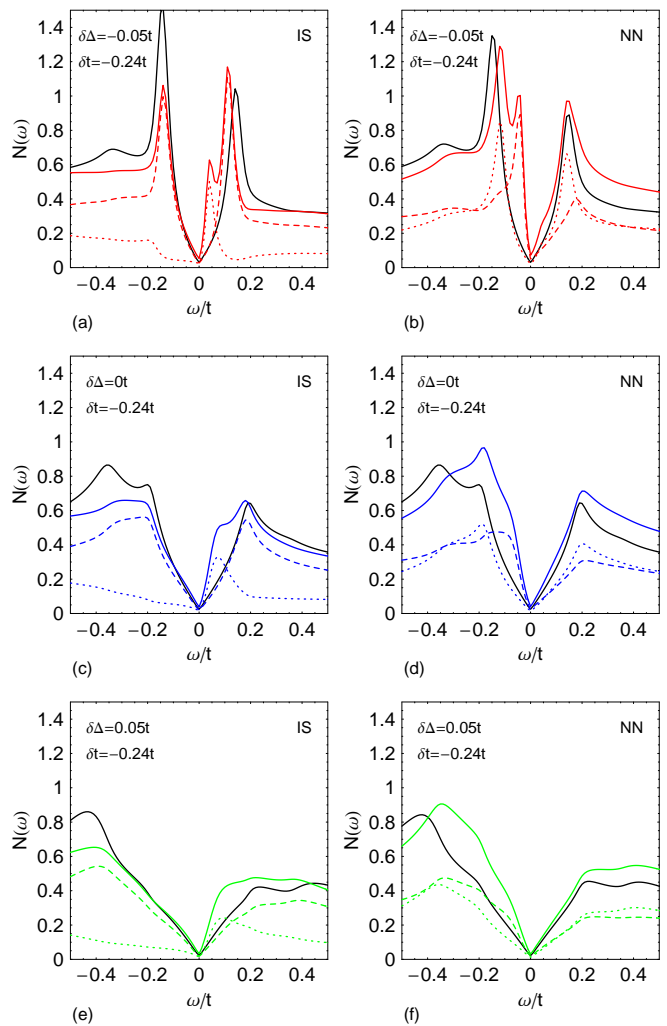


FIG. 3: (Color online) Same as Fig. 2 but including local impurity-induced reduced hopping $\delta t = -0.24t$.

effective hopping found in recent studies of impurities in a host described by the $t - t' - J$ model.³⁹ Note this is an atomic scale modulation caused by the in-plane impurity due solely to magnetic correlations in the host. By contrast, we also study a modulation of the order parameter, but assume that this is caused by an out-of-plane influence such as a dopant atom, which gives rise to a patch of modulated $\Delta_{\mathbf{k}}$ of roughly 20 \AA . Thus we study the impurity added to a patch of reduced or enhanced $\Delta_{\mathbf{k}}$ on a 5×5 square as shown in Fig. 1 embedded in an infinite system of fixed order parameter Δ_0 .

III. Ni IMPURITY

We first discuss the case of magnetic impurity ions such as Ni. In Fig. 2 we show the LDOS at the magnetic impurity site using the parameters $V_3 = -0.8t, V_0 = 0.6t$, and $\delta\Delta = -0.05t, 0, +0.05t$ corresponding to a local suppressed, constant, and enhanced gap patch, respectively.

The \mathcal{T} -matrix corresponding to this potential has a pole at an energy $\Omega_0 \sim 0.05t$, but, as is evident from Fig. 2, resonance are visible neither on the impurity site (IS) nor on the nearest neighbor (NN) site. Note that while in Fig. 2 we have assumed a quasiparticle scattering rate $\Gamma(\omega) = 0.1|\omega|$ similar to that observed in experiment⁴⁰, the absence of resonance features is not caused by this broadening. Instead, it is the fact that the coupling to the continuum at Ω_0 is simply too strong. In Fig. 3, we show the same sites with the same potentials in a situation where the hopping has been reduced around the Ni impurity; it is clear that the resonance is observable, and corresponds very closely in energy and weight to experiment.¹³ It appears, however, only in the case where the order parameter has been suppressed [Fig. 3(a,b)] over a patch, thus creating the sharp coherence peaks which are then separated from the impurity feature. At this point, the role of the suppressed hopping is purely phenomenological, but we note that such a reduction was also assumed in the more complicated set of potential parameters taken by Tang and Flatté¹⁴ to describe the Ni resonance. The particular values of δt and $\delta\Delta$ necessary for the LDOS near the Ni impurity to resemble the experimental data are bandstructure-dependent.

From the point of view of experiment, scanning at a bias voltage corresponding to the resonant frequency $\omega = \pm\Omega_0$ of the Ni resonance should produce spatial patterns as shown in Fig. 4. In the left column of panels, we show the LDOS at resonance without suppressed hopping; impurity states are hardly observable, even in the reduced gap case. When the hopping around the impurity site is reduced, the pattern is clearly seen in the suppressed gap case but not in the large gap case. Note that the images at positive and negative bias show fourfold patterns which are rotated by 45° with respect to each other, as observed in experiment¹¹ and earlier theories.^{14,15}

IV. Zn IMPURITY

The LDOS pattern predicted for an unitary scatterer in a d -wave superconductor with noninteracting quasiparticles is well-known to have crucial qualitative differences with the measured STS conductance maps $G(eV, \mathbf{r})$, at least if these are interpreted in the usual way as being directly proportional to the LDOS. The primary discrepancy is the existence of an observed intensity maximum on the central site of the impurity pattern in the case of Zn, which is impossible in the naive theory for potentials V_3 larger than the bandwidth, since electrons are effectively excluded from this site. There have been several theoretical approaches to understand this apparent paradox. The first is specific to the STM method and relies on the fact that the impurity states are localized in the CuO_2 plane, two layers below the BiO surface probed by the STM tip; the intervening layers are then argued to provide a blocking layer-specific tunneling path

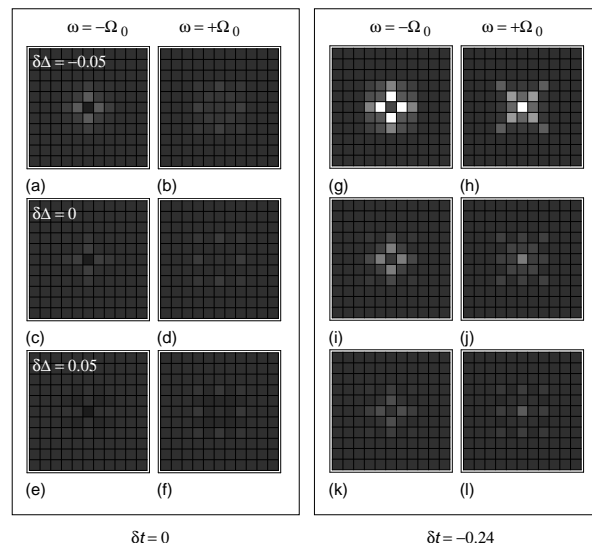


FIG. 4: LDOS real-space pattern $N(\mathbf{r}, \pm\Omega_0)$ at the resonance frequency for Ni impurities modelled as described in the text. Left panel: no suppression of hopping by impurity assumed. Subpanels (a-b), (c-d), and (e-f) show the resonance pattern for gap sizes in the surrounding 5×5 patch corresponding to $\delta\Delta = +0.05t, 0$, and $-0.05t$, respectively. Left column (a,c,e) and right column (b,d,f) correspond to negative and positive resonance frequency $\pm\Omega_0$, respectively. Right panel: same as left panel but for including additional modulations of the hopping $\delta t = -0.24t$.

which samples not the Cu directly below the tip, but preferentially the four nearest neighbors.^{41,42} Some indirect support for this point of view has been provided by density functional theory,⁴³ which finds that the pattern of LDOS near the impurity but close to the BiO surface can be quite different than the LDOS in the CuO_2 plane. On the other hand, this calculation, applicable only to the normal state, suggested that the hybridization of the wavefunctions involved is not only blocking layer-specific, but also specific to the particular chemical impurity in question. A second class of approaches obtains LDOS patterns similar to experiment for both Zn and Ni by simply assuming an *ad hoc* distribution of site potentials and nearby hoppings to tune the weights of on-site and nearest-neighbor LDOS.^{14,44} While the bare impurity potential has a much shorter range of order $\sim 1\text{\AA}$ ⁴³ compared to this ansatz, it is possible that the phenomenological parameters used in these models represent dynamically generated quantities in a more complete theory. Finally, the observed Zn conductance pattern has also been obtained in theories which describe the Zn as a Kondo impurity¹⁶ and pairing impurity,¹⁸ respectively. We now discuss each of these scenarios in the context of the resonance extinction problem.

A. Zn as Kondo impurity

Motivated by NMR measurements^{45–49} showing that nonmagnetic Zn impurities induce a local spin 1/2 in their vicinity, it was proposed that the LDOS data could be understood within a nonlocal Kondo model.^{16,50} With a proper choice of a large magnetic potential coupling the nonlocal spin associated with the impurity to the conduction electron bath, the observed spatial pattern could be reproduced. This requires, however, the assumption of a very weak potential scattering at the Zn site. An interpretation of this work accounted also for the disappearance of impurity resonances in large-gap patches^{16,19} by assuming that such regions were underdoped and therefore poorly screened. In such a case, the Kondo temperature T_K would fall below the measurement temperature, leaving the impurity in the local moment (nonresonant) regime. More recently, however, it has been observed by STM that spatial charge variations are in fact quite small, of order a few percent, and that the presence of dopants *correlates* (rather than anticorrelates) with the large-gap regions.²⁵ In addition, resonances that have been observed in underdoped samples at temperatures well above the Kondo temperature expected from NMR¹⁷ are similar to the low temperature impurity spectra.^{13,22,51} Nevertheless, recently Kirćan proposed a mechanism by which the size of the superconducting gap can modify the impurity moment exchange coupling to the d -wave quasiparticle bath.²⁴ In the large-gap regions, states are pushed further away from the Fermi level, thus decreasing the ability of the quasiparticle system to screen the impurity, leading to a lower T_K . This does not appear to address the set of critiques above, but is consistent with the STM results on BSCCO at low T . We return to this scenario below, after discussing other possibilities.

B. Zn as screened Coulomb impurity

We now examine the conventional point of view that, since Zn^{2+} is a closed shell ion, it creates a strong localized screened Coulomb potential⁴³ in a BSCCO host. A strong impurity potential of this type is typically represented as a δ -function potential in the Hamiltonian with $V_3 \gg t$ and $V_0 = 0$ in the notation of Eq.(3), and it is well-known that such a perturbation generates an in-gap resonant state in a d -wave superconductor.⁵² In a particle-hole symmetric normal state band, this LDOS resonance can be tuned to $\Omega_0 = 0$ with $V_3 = \infty$, but in a more general band a specific fine-tuned value of the potential is required to produce a resonance at zero energy (unitarity) or any other particular subgap energy.^{53,54} For the band we have adopted here, which roughly reproduces the correct Fermi surface of optimally doped BSCCO, tuning the resonance to the nominal resonance frequency observed by STS¹² of $\Omega_0 \simeq -2\text{meV} \simeq 0.013t$ requires a potential of approximately $V_3 = 2.5t$. In Fig. 5, we have plotted the resonance arising from such a poten-

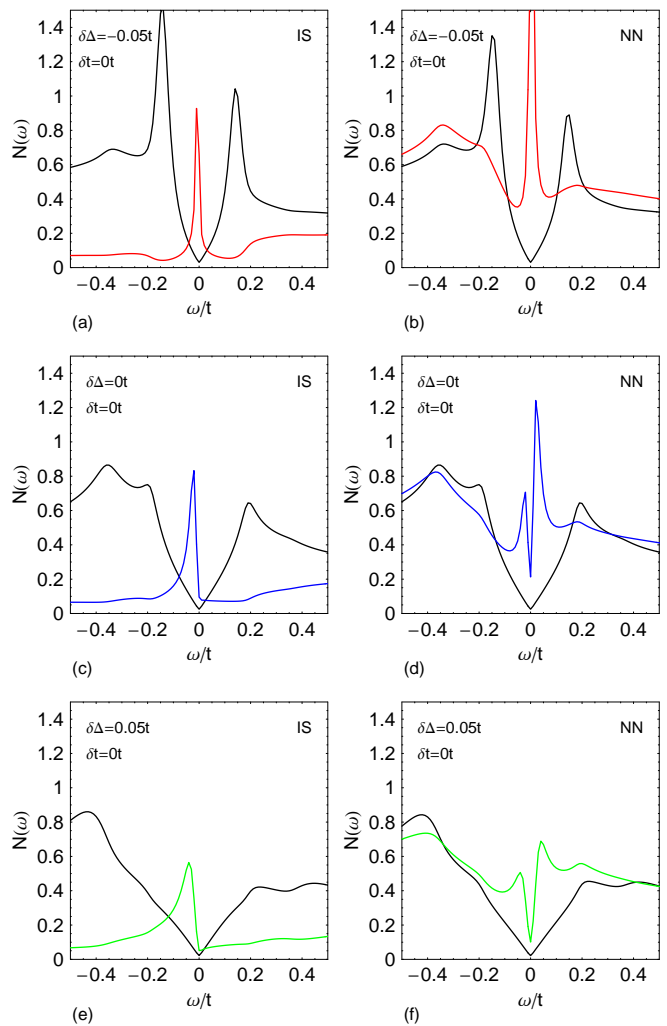


FIG. 5: (Color online) LDOS at impurity site (IS) and nearest neighbor sites (NN) plotted in left and right panels respectively for various gap modulations $\delta\Delta = -0.05t, 0, +0.05t$ over a 5×5 patch around the impurity, described by an on-site potential $V_3 = 2.5t$. Black curves show the LDOS in the absence of an impurity, while colored curves correspond to the situation where an impurity is present. Hoppings are not modulated, $\delta t = 0$

tial on both the impurity site (IS) and nearest neighbor site (NN), for various values of the gap size in the local patch around the impurity, as for the Ni case. There are two obvious difficulties. The first is the well-known problem discussed above, that the intensity on the IS is substantially smaller than on the NN site, in contradiction to experiment. The second problem relates to the behavior of the resonance in different types of local patches. The resonance is suppressed somewhat in the large-gap regions corresponding to Fig. 5(e-f), but is still clearly visible. In fact, it is clear that the gap modulation $\delta\Delta$ has simply detuned the resonance and acts, via its coupling through the T -matrix equations to the diagonal channel, as a renormalization of the impurity potential.

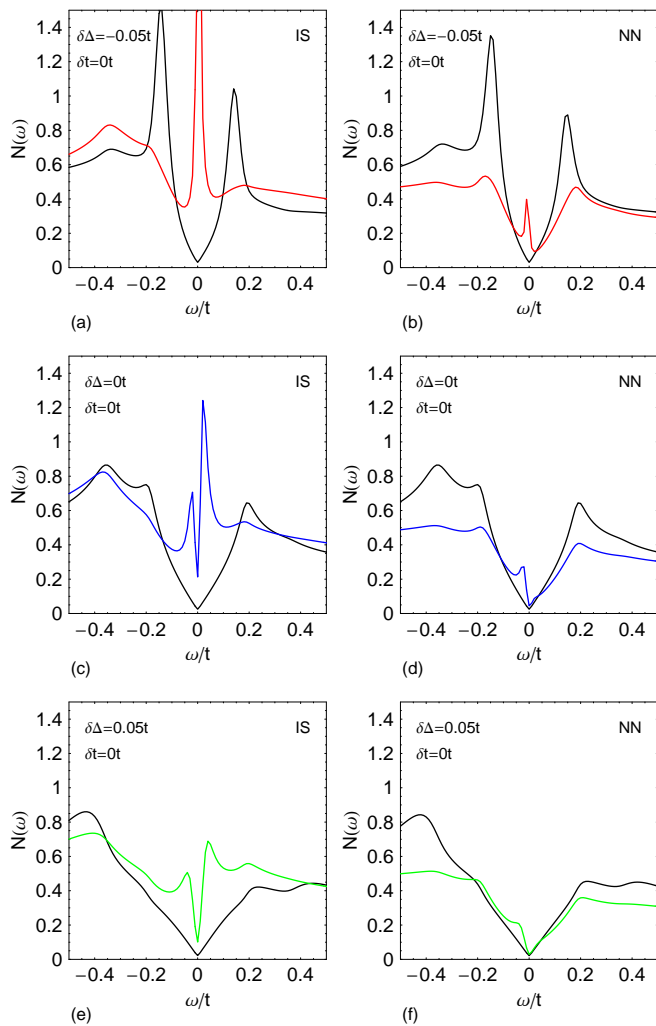


FIG. 6: (Color online) Same as Fig. 5, but with a filter mechanism applied as described in text.

The clear splitting of the resonance and shift of the peak with increasing $\delta\Delta$ is obvious in panels (b,d,f). The inability of the conventional screened Coulomb model for Zn to explain the real disappearance of the resonances in the large-gap regions with this scenario was emphasized recently by Kircan,²⁴ who studied a similar model.

We now recall that the correct spatial pattern can be recovered by employing the assumption of a blocking layer “filter”,^{41,42} which supposes that the tunneling path to the CuO₂ plane is not direct. We employ the simplest of these approaches,⁴¹ which assumes that the LDOS measured on any given site is actually the average of the LDOS on the four NN sites. In this case, as seen from Fig. 6 the correct spatial pattern is recovered,¹⁵ and one sees that the resonance in the large-gap regions is in fact hardly observable, particularly if one searches for such objects by looking for values of the 0 meV conductance which exceed the noise threshold, as in Ref. 19. Of course, applying the same filter mechanism to the Ni pattern will spoil the good agreement, so one is left with

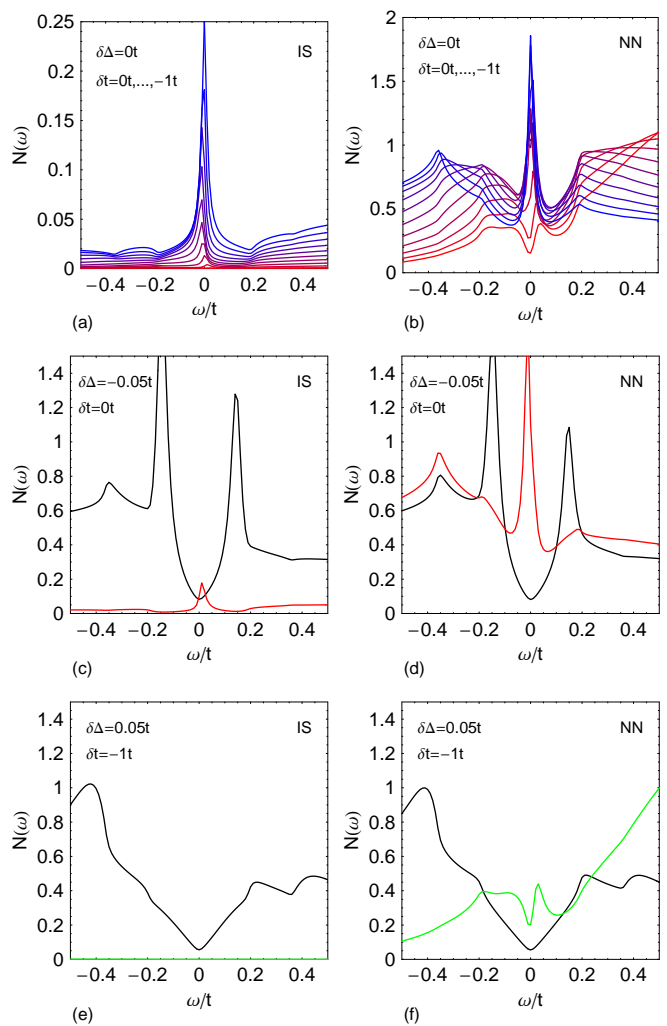


FIG. 7: (Color online) LDOS for a Zn impurity represented by a potential $V_3 = 5t$ and calculated with a constant scattering rate $\eta = 0.01t$ where the hopping is suppressed using a Gaussian distribution with the maximum δt on the four bonds around the impurity, and a decay length of one lattice spacing. (a,c,e) show the LDOS at the IS site and (b,d,f) at the NN site. (a) and (b) show the LDOS in a region of constant gap ($\delta\Delta = 0$) for different hopping suppression where the values of δt shown vary from 0 (top) to $-t$ (bottom) in steps of $-0.1t$. (c) and (d) show the LDOS in a small-gap region without suppression of the hopping while (e) and (f) show it in large-gap region with maximum suppression of the hopping ($\delta t = -t$).

the unpleasant alternative of arguing that the effect of the intervening layers may be different in the case of the two impurities. This was in fact the conclusion reached by Ref. 43, but it destroys the utility of comparing the patterns for the two species as a way to extract information.

The resonances observed in Fig. 6(e) still appear as small peaks in the LDOS at a shifted energy, and so might be observable; the case for such a scenario re-

ally eliminating the resonances in the large-gap regions is therefore not completely convincing. Before leaving this scenario, therefore, we discuss briefly the case of reduced hopping. We remind the reader that due to the antiferromagnetic correlations in the host material, the hopping is expected to be reduced over the antiferromagnetic correlation length, of order a few lattice spacings.³⁹ This renormalization might be expected to be more important in the case of Zn than Ni, due to the stronger bare potential.⁴³ We therefore plot in Fig. 7(a,b) the resonance in a homogeneous background order parameter ($\delta\Delta = 0$) for various values of the hopping near the impurity. It is seen that the reduced hopping dramatically suppresses the weight in the impurity resonance on both the impurity [Fig. 7(a)] and NN [Fig. 7(b)] sites, which is lost to the antibound state outside the band. The resonance position will shift somewhat, however, since the effective potential for the impurity which enters in the determinant of the T -matrix is changing. As shown in Fig. 7(c-f), assuming a sufficiently large renormalized hopping in large-gap regions, it is possible to completely wipe-out what would be a well-defined sharp resonance in a small-gap region. Thus, provided the experimental data are consistent with individual Zn's displaying small shifts in the resonance position in intermediate strength gap patches, the conventional scenario reviewed in the section, modified by kinetic energy renormalization from electronic correlations, may well be consistent with the data.

C. Zn as phase impurity

One of the more exotic proposals to describe the LDOS measurements near Zn impurities is the so-called phase

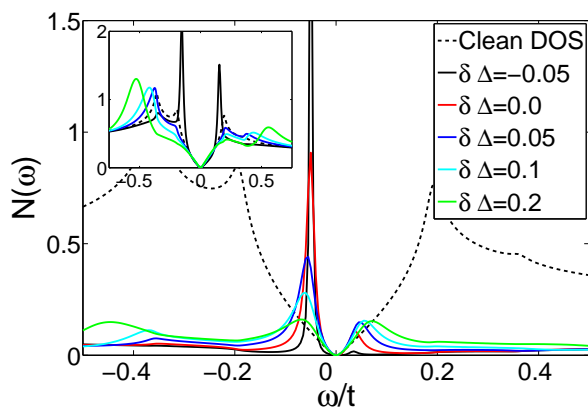


FIG. 8: (Color online) LDOS of a phase impurity with $\alpha = 1.5$ as a function of the change in the local gap $\delta\Delta$ within the 5×5 patch in which it lies. The red curve is similar to the results in Ref. 18, which reported the LDOS near a phase impurity in a homogeneous superconductor. The inset shows the LDOS without the phase impurity (same color code).

impurity scenario.¹⁸ As was shown in Ref. 18, local sign changes of the pairing amplitude on the four nearest bonds to the impurity site can generate low-energy Andreev resonant states with the correct real-space distribution (without a filter mechanism). This is true only for a sufficiently small conventional impurity potential (see Ref. 18 for details).¹⁸ Using the same notation as in Ref. 18, we introduce the parameter α which sets the strength of the phase impurity by adding a potential in the τ_1 Nambu channel of $V_1 = -\alpha\Delta_0$ which affects only the four NN bonds to the impurity site in the center of the 5×5 patch. As α increases, the Andreev resonance moves to lower energy and sharpens up, and the resonance energy Ω_0 can approach zero when α becomes greater than 1. This means that the order parameter actually changes its phase by π on an atomic scale. The question relevant to the present study is how these Andreev states depend on the local gap patch in which they are positioned. In order to answer this, we have studied the LDOS near phase impurities with $\alpha = 1.5$ in the center of gap patches of size 5×5 . Assuming that Zn causes the same local changes of the gap irrespective of the local gap environment (i.e. same α for all local gap values of the 5×5 patch), then one would expect sharper resonances in small-gap regions since there the phase impurity is effectively stronger. Indeed, the special case of a phase impurity of strength α in a large-gap region with increased local gap also of size α has effectively no phase impurity at all, and hence no low-energy resonance.

In Fig. 8 we show the LDOS at the center of the phase impurity as a function of the local gap change $\delta\Delta$ in the 5×5 gap patch. As expected, small-gap regions support well-defined Andreev resonant states, which are however much weaker in large-gap regions. Thus at least at a qualitative level the phase impurity scenario seems to be fully consistent with the present experimental STM data near Zn impurities. Note that the results in Fig. 8 are shown without the filter effect, and with $\delta t = 0$ and a constant smearing factor $\eta = 0.01t$ as opposed to an inelastic scattering rate $\Gamma(\omega) = 0.1|\omega|$ used in Figs. 2-6. We find that local suppression of the hopping mainly renormalizes α ($\delta t < 0$ leads to smaller effective α) whereas $\Gamma(\omega)$, which dominates the large-gap regions,⁴⁰ obviously leads to further smearing preferentially of the high-energy features $\omega \gtrsim \Delta$.

V. DISCUSSION

Several rather general points and caveats need to be mentioned in connection with the overall problem. First, we have assumed that the impurity resonances are extinguished because of some effect of the electronic system, i.e. we ignore the possibility that the impurities themselves are simply absent due to nonrandom processes during the crystal growth (for a discussion, see Ref. 19).

Second, we have assumed that the spectral gap is a quantity characterizing the strength of the same elec-

tronic state in all gap patches. Clearly, if the large-gap patches even at optimal doping correspond to a competing electronic state, a very different approach is necessary. The naïve proposal that these gap patches correspond to pseudogap regions does not, however, suffice to explain the absence of impurity resonances, since most models of the pseudogap state allow for such resonances,^{20,55–57} and in addition, by heating the sample through T_c , they have now been observed to survive well in to the pseudogap state.²¹ The Gaussian distribution of gap sizes observed by STS also suggests that there is no qualitative difference between, e.g. large-gap regions and intermediate-gap regions.

Third, we note that all our calculations (and those of others) have been performed for models of a single impurity in some realization of a d -wave superconductor. In the real many-impurity problem, interference between different impurity resonances leads to distortions of fourfold symmetry and shifts of resonance energies.^{36–38} These effects are particularly strong for near-unitary scatterers like Zn.⁵⁸ Direct comparison of a single experimental spectrum with a 1-impurity theoretical prediction are therefore generally problematic. It is likely that these effects are responsible for the fact that the existing experimental data (for fields of view imaged by STS containing tens of impurities) for resonance strength versus gap size are extremely noisy¹⁹ and show no clear evidence for a continuous suppression of the resonance peak as the local gap size is increased, a characteristic of *all* the theoretical models discussed here. Improving these statistics, with hundreds rather than tens of impurities, and binning over a range of gap sizes, should enable more robust conclusions to be drawn. According to Ref. 58, some of the effects of interference may also be minimized by defining the strength of the resonance via an integral over a small energy window near the peak rather than simply by the value of the conductance at a fixed bias.

Fourth, both the Kondo scenario and the phase impurity scenario produce the same spatial pattern for the Zn resonance as observed in experiment, whereas the screened Coulomb impurity picture requires an assumption of a filter mechanism. If the existence or nonexistence of such a mechanism could be settled in the case of the small-gap regions, it would enable one to rule out at least one candidate. Refs. 18 and 37 proposed that this could be settled if one can find isolated pairs of resonances in the same gap region.

Fifth, we discuss how the different scenarios for Zn can be distinguished, independent of filter mechanism. If truly isolated resonances were available, the shift of resonance positions from patch to patch could suffice to single out the model with Zn as a screened Coulomb scatterer. However, as discussed above, interference effects will likely induce such shifts in either of the remaining scenarios as well.

The Kondo scenario for the Zn moment can be tested by a systematic measurement of the T -dependence of the impurity resonances. According to Kircàn,²⁴ the effective

Kondo scale depends on the gap size. Since the measured distribution of gaps is continuous, it should be possible to find resonances in intermediate-gap regions characterized by a small enough Kondo scale, such that the resonance will disappear with increasing temperature, still in the superconducting state. In the conventional scenarios, or in non-Kondo scenarios where the observed moment is due to background correlations in the host system, increasing temperature should broaden but not eliminate the resonance until the gap disappears.

Another method to distinguish these scenarios is to apply a magnetic field. In a magnetic field, resonances due to an ordinary potential will be split by a Zeeman coupling⁵⁹ linearly in the magnetic field strength. Splitting of the resonance peak also characterizes the phase impurity and the Kondo resonance in a magnetic field. However, as shown in Ref. 60, deviations from the linear Zeeman splitting characterizes the Kondo resonance as the field becomes of order the Kondo temperature and the two split peaks develop a strong asymmetry in their weight. For the intermediate gap patches with $T_K \ll T_c$ discussed above, the corresponding field scale where the crossover occurs should be small enough such that the unusual field dependence predicted in Ref. 60 should become observable.

Sixth, we remind the reader that none of the models discussed here incorporate systematically the effects of the approach to the Mott transition on the underdoped side. We have attempted to include the correlation-induced band narrowing near an impurity due to correlations in a phenomenological way, but a more complete treatment is clearly desirable.

Finally, we address the question of the static local moment induced by Zn in the underdoped regime.⁶¹ In the conventional model discussed above, such a moment is not included in the theory. Recent studies however, have extended this scenario (extended conventional scenario) by including Hubbard correlations U in the host superconductor, and found that nonmagnetic scatterers can indeed generate—for sufficiently strong correlations—a local $S = 1/2$ state tied to the impurity site,^{62,63} in agreement with results obtained from the $t - J$ model treated in the slave-boson mean-field⁶⁴ or Gutzwiller approximation.⁶⁵ An important property of the LDOS resonance within the latter scenario is that it is intrinsically split by the local moment whereas no such effect exists in zero field within the Kondo approach. Therefore, experimental observation of thermally broadened resonances which split in zero field as the temperature is lowered would be strong support for the extended conventional scenario. We stress that local inhomogeneity may cause some resonances to exhibit this behavior while others will not.

VI. CONCLUSIONS

In this paper we have investigated a number of scenarios which might explain why STS experiments fail to

observe Ni and Zn resonances in large-gap regions of the BSCCO superconductors. In the case of Ni, it appears that the physics of an inhomogeneous d -wave superconductor alone suffices to explain the phenomenon. That is, only in the case of a coherence-length size small-gap region embedded in a larger gap region can one expect to have sufficiently sharp and strong features at the nominal gap positions for the impurity resonance to borrow enough weight for it to be well-defined. This is a direct consequence of Andreev states formed by partially trapped quasiparticles in suppressed order parameter regions, as pointed out by Nunner *et al.*²⁶ and Fang *et al.*³⁵

In discussing the similar question for the Zn resonances, we considered several scenarios. The first, due to Kirčan, assumes that the resonance is formed primarily due to Kondo screening of the magnetic moment formed in the correlated system around the Zn site, and proposes that in the large-gap regions the moment is free (unscreened). This seems unlikely to us, given that no temperature dependence of these resonances has been observed other than thermal broadening,^{21,22} but we have proposed further tests that should clarify this issue. The second scenario is similar to the physics of the extinction of the Ni resonances: if the mobility of quasiparticles is reduced in the vicinity of the Zn due to correlations, the resonance will be suppressed as the size of the order parameter in the patch is increased, but shifted as well. This scenario cannot presently be ruled out by existing data. Finally, if the Zn ion primarily influences the pair field locally, such as to cause a local π phase shift of

the order parameter, it will produce a resonance whose weight depends directly on the size of the local gap, and vanishes in sufficiently large gap regions.

Further theoretical and experimental work is clearly necessary to answer the very fundamental challenge posed here. From the theoretical side, we have included strong electronic correlations only in a very phenomenological way, by introducing local suppressions of the hole mobility around the impurity site, as found by more sophisticated treatments in the normal state.³⁹ As these effects appear to be important, theoretical treatments of impurities in the superconducting state capable of treating inhomogeneous order parameter situations together with strong correlations are clearly desirable. On the experimental side, we have discussed ways in which improving statistics on impurity resonances and how they are defined could provide important insights, and proposed various tests of the scenarios treated here which should enable one to distinguish them.

VII. ACKNOWLEDGEMENTS

The authors are grateful for discussions with J.C. Davis, M. Vojta, and W. Chen. P.J.H. and S.G. were funded by DOE Grant DE-FG02-05ER46236 and S.G. acknowledges support by the Deutsche Forschungsgemeinschaft. B.M.A. acknowledges support from the Villum Kann Rasmussen foundation.

-
- ¹ P. A. Lee, N. Nagaosa, and X.-G. Wen, *Rev. Mod. Phys.* **78**, 17 (2006).
- ² S. A. Kivelson, I. P. Bindloss, E. Fradkin, V. Oganesyan, J. M. Tranquada, A. Kapitulnik, and C. Howald, *Rev. Mod. Phys.* **75**, 1201 (2003).
- ³ G. Alvarez, M. Mayr, A. Moreo, and E. Dagotto, *Phys. Rev. B* **71**, 014514 (2005); M. Mayr, G. Alvarez, A. Moreo, and E. Dagotto, *Phys. Rev. B* **73**, 014509 (2006).
- ⁴ B. M. Andersen, P. J. Hirschfeld, A. P. Kampf, and M. Schmid, *Phys. Rev. Lett.* **99**, 147002 (2007).
- ⁵ W. A. Atkinson, *Phys. Rev. B* **75**, 024510 (2007).
- ⁶ B. M. Andersen and P. J. Hirschfeld, *Phys. Rev. Lett.* **100**, 257003 (2008).
- ⁷ G. Alvarez and E. Dagotto, arXiv:0802.3394v1.
- ⁸ T. Cren, D. Roditchev, W. Sacks, J. Klein, J.-B. Moussy, C. Deville-Cavellin, and M. Laguës, *Phys. Rev. Lett.* **84**, 147 (2000).
- ⁹ C. Howald, P. Fournier, and A. Kapitulnik, *Phys. Rev. B* **64**, 100504 (2001).
- ¹⁰ S. H. Pan, J. P. O’Neal, R. L. Badzey, C. Chamon, H. Ding, J. R. Engelbrecht, Z. Wang, H. Eisaki, S. Uchida, A. K. Gupta, K.-W. Ng, E. W. Hudson, K. M. Lang, and J. C. Davis, *Nature (London)* **413**, 282 (2001).
- ¹¹ K. M. Lang, V. Madhavan, J. E. Hoffman, E. W. Hudson, H. Eisaki, S. Uchida, and J. C. Davis, *Nature (London)* **415**, 412 (2002).
- ¹² S. H. Pan, E. W. Hudson, K. M. Lang, H. Eisaki, S. Uchida, and J. C. Davis, *Nature (London)* **403**, 746 (2000).
- ¹³ E. Hudson, K. M. Lang, V. Madhavan, S. H. Pan, H. Eisaki, S. Uchida, and J. C. Davis, *Nature (London)* **411**, 920 (2001).
- ¹⁴ J.-M. Tang and M. E. Flatté, *Phys. Rev. B* **66**, 060504 (2002).
- ¹⁵ A. V. Balatsky, I. Vekhter, and J.-X. Zhu, *Rev. Mod. Phys.* **78**, 373 (2006).
- ¹⁶ A. Polkovnikov, S. Sachdev, and M. Vojta, *Phys. Rev. Lett.* **86**, 296 (2001).
- ¹⁷ H. Alloul, J. Bobroff, M. Gabay, and P. J. Hirschfeld, arXiv:0711.0877v1.
- ¹⁸ B. M. Andersen, A. Melikyan, T. S. Nunner, and P. J. Hirschfeld, *Phys. Rev. Lett.* **96**, 097004 (2006).
- ¹⁹ J. Hoffman, Ph.D. thesis, University of California-Berkeley thesis, 2003.
- ²⁰ H. V. Kruijs, I. Martin, and A. V. Balatsky, *Phys. Rev. B* **64**, 054501 (2001).
- ²¹ K. Chatterjee, M. C. Boyer, W. D. Wise, T. Kondo, T. Takeuchi, H. Ikuta, and E. W. Hudson, *Nature Phys.* **4**, 108 (2008).
- ²² H. Kambara, Y. Niimi, M. Ishikado, S. Uchida, and H. Fukuyama, *Phys. Rev. B* **76**, 052506 (2007).
- ²³ J. C. Davis, private communication.
- ²⁴ M. Kirčan, *Phys. Rev. B* **77**, 214508 (2008).

- ²⁵ K. McElroy, Jinho Lee, J. A. Slezak, D.-H. Lee, H. Eisaki, S. Uchida, and J. C. Davis, *Science* **309**, 1048 (2005).
- ²⁶ T. S. Nunner, B. M. Andersen, A. Melikyan, and P. J. Hirschfeld, *Phys. Rev. Lett.* **95**, 177003 (2005).
- ²⁷ T. S. Nunner, P. J. Hirschfeld, B. M. Andersen, A. Melikyan, and K. McElroy, *Physica C*, **460-462**, 446 (2007).
- ²⁸ T. S. Nunner, W. Chen, B. M. Andersen, A. Melikyan, and P. J. Hirschfeld, *Phys. Rev. B* **73**, 104511 (2006).
- ²⁹ K. McElroy, R. W. Simmonds, J. E. Hoffman, D.-H. Lee, J. Orenstein, H. Eisaki, S. Uchida, and J. C. Davis, *Nature (London)* **422**, 592 (2003).
- ³⁰ J. A. Slezak, Jinho Lee, M. Wang, K. McElroy, K. Fujita, B. M. Andersen, P. J. Hirschfeld, H. Eisaki, S. Uchida, and J. C. Davis, *Proc. Natl. Acad. Sci. USA* **105**, 3203 (2008).
- ³¹ B. M. Andersen, P. J. Hirschfeld, and J. A. Slezak, *Phys. Rev. B* **76**, 020507 (2007).
- ³² K. K. Gomes, A. N. Pasupathy, A. Pushp, S. Ono, Y. Ando, and A. Yazdani, *Nature (London)* **447**, 569 (2007).
- ³³ B. M. Andersen, A. Melikyan, T. S. Nunner, and P. J. Hirschfeld, *Phys. Rev. B* **74**, 060501 (2006).
- ³⁴ J. W. Loram and J. L. Tallon, arXiv:cond-mat/0609305v1.
- ³⁵ A. C. Fang, L. Capriotti, D. J. Scalapino, S. A. Kivelson, N. Kaneko, M. Greven, and A. Kapitulnik, *Phys. Rev. Lett.* **96**, 017007 (2006).
- ³⁶ D. K. Morr and N. A. Stavropoulos, *Phys. Rev. B* **66**, 140508 (2002).
- ³⁷ L. Zhu, W. A. Atkinson, and P. J. Hirschfeld, *Phys. Rev. B* **67**, 094508 (2003).
- ³⁸ B. M. Andersen and P. Hedegård, *Phys. Rev. B* **67**, 172505 (2003).
- ³⁹ M. Gabay, P. J. Hirschfeld, E. Semel, and W. Chen, *Phys. Rev. B* **77**, 165110 (2008).
- ⁴⁰ J. W. Alldredge, Jinho Lee, K. McElroy, M. Wang, K. Fujita, Y. Kohsaka, C. Taylor, H. Eisaki, S. Uchida, P. J. Hirschfeld, and J. C. Davis, *Nature Phys.* **4**, 319 (2008).
- ⁴¹ J.-X. Zhu, C. S. Ting, and C. R. Hu, *Phys. Rev. B* **62**, 6027 (2000).
- ⁴² I. Martin, A. Balatsky, and J. Zaanen, *Phys. Rev. Lett.* **88**, 097003 (2002).
- ⁴³ L.-L. Wang, P. J. Hirschfeld, and H.-P. Cheng, *Phys. Rev. B* **72**, 224516 (2005).
- ⁴⁴ J.-M. Tang and M. Flatté, *Phys. Rev. B* **70**, 140510 (2004).
- ⁴⁵ H. Alloul, P. Mendels, H. Casalta, J. F. Marucco, and J. Arabski, *Phys. Rev. Lett.* **67**, 3140 (1991).
- ⁴⁶ A. V. Mahajan, H. Alloul, G. Collin, and J. F. Marucco, *Phys. Rev. Lett.* **72**, 3100 (1994).
- ⁴⁷ J. Bobroff, W. A. MacFarlane, H. Alloul, P. Mendels, N. Blanchard, G. Collin, and J.-F. Marucco, *Phys. Rev. Lett.* **83**, 4381 (1999).
- ⁴⁸ P. Mendels, J. Bobroff, G. Collin, H. Alloul, M. Gabay, J. F. Marucco, N. Blanchard, and B. Grenier, *Europhys. Lett.* **46**, 678 (1999).
- ⁴⁹ M.-H. Julien, T. Fehér, M. Horvatić, C. Berthier, O. N. Bakharev, P. Ségransan, G. Collin, and J.-F. Marucco, *Phys. Rev. Lett.* **84**, 3422 (2000).
- ⁵⁰ M. Vojta and R. Bulla, *Phys. Rev. B* **65**, 014511 (2001).
- ⁵¹ M. Vershinin, S. Misra, S. Ono, Y. Abe, Y. Ando, and A. Yazdani, *Science* **303**, 1995 (2004).
- ⁵² A. V. Balatsky, M. I. Salkola, and A. Rosengren, *Phys. Rev. B* **51**, 15547 (1995).
- ⁵³ R. Joynt, *J. Low Temp. Phys.* **109**, 811 (1997).
- ⁵⁴ W. A. Atkinson, P. J. Hirschfeld and A. H. MacDonald, *Physica C* **341-348**, 1687 (2000).
- ⁵⁵ Q.-H. Wang, *Phys. Rev. Lett.* **88**, 057002 (2002).
- ⁵⁶ D. K. Morr, *Phys. Rev. Lett.* **89**, 106401 (2002).
- ⁵⁷ B. M. Andersen, *Phys. Rev. B* **68**, 094518 (2003).
- ⁵⁸ W. A. Atkinson, P. J. Hirschfeld, and L. Zhu, *Phys. Rev. B* **68**, 054501 (2003).
- ⁵⁹ C. Grimaldi, *Phys. Rev. B* **65**, 094502 (2002).
- ⁶⁰ M. Vojta, R. Zitzler, R. Bulla, and T. Pruschke, *Phys. Rev. B* **66**, 134527 (2002).
- ⁶¹ C. Panagopoulos, J. L. Tallon, B. D. Rainford, T. Xiang, J. R. Cooper, and C. A. Scott, *Phys. Rev. B* **66**, 064501 (2002).
- ⁶² Y. Chen and C. S. Ting, *Phys. Rev. Lett.* **92**, 077203 (2004).
- ⁶³ J. W. Harter, B. M. Andersen, J. Bobroff, M. Gabay, and P. J. Hirschfeld, *Phys. Rev. B* **75**, 054520 (2007).
- ⁶⁴ Z. Wang and P. A. Lee, *Phys. Rev. Lett.* **89**, 217002 (2002).
- ⁶⁵ H. Tsuchiura, Y. Tanaka, M. Ogata, and S. Kashiwaya, *Phys. Rev. B* **64**, 140501 (2001).